PEG-IFN/RBV). Further studies are needed to clarify the significance of the core mutations for final outcome of the treatment in the context of the HCV genome-wide analysis.

Different viral responses by polymorphisms in core 70 were also recently suggested in North American patients by Donlin et al. [7]. However, it was reported that the association with core 70 was weaker in their study. Very recently, the IL28B (interferon-lambda-3) gene polymorphism has been found to be closely associated with treatment response in patients in the United States, European Union and Japan by human genome-wide analysis [8–10]. The favorable IL28B genotype is found most frequently in Asian patients, second in European-Americans, and least in African-Americans, indicating that a well-known racial difference in treatment efficacy can be explained by the IL28B polymorphism. The interaction between viral and human genome polymorphisms should be studied further with regard to the treatment response.

## Conclusion

HCV genome-wide analysis with a large number of patients successfully revealed that core 70 and NS5A are the most important factors determining the virological kinetics during PEG-IFN/RBV therapy. Viral genome-wide analysis is a promising tool for elucidating the unknown viral factors for different pathological pictures, such as disease progression.

## Disclosure Statement

Supported in part by a Grant-in-Aid for Research on Hepatitis (grant ID H19-002) from the Ministry of Health, Labor, and Welfare, Japan. The authors report receiving grant support from Schering-Plough and Roche.

## References

1 Neumann AU, Pianko S, Zeuzem S, Yoshida EM, Benhamou Y, Mishan M, et al: Positive and negative prediction of sustained virologic response at weeks 2 and 4 of treatment with albinterferon alfa-2b or peginterferon alfa-2a in treatment-naive patients with genotype 1, chronic hepatitis C. J Hepatol 2009; 51:21–28.

2 Lee SS, Ferenci P: Optimizing outcomes in patients with hepatitis C virus genotype 1 or 4. Antivir Ther 2008;13(suppl 1):9–16.

3 Enomoto N, Sakuma I, Asahina Y, Kurosaki M, Murakami T, Yamamoto C, et al: Comparison of full-length sequences of interferon-sensitive and resistant hepatitis C virus 1b: sensitivity to interferon is conferred by amino acid substitutions in the NS5A region. J Clin Invest 1995;96:224–230.

4 Enomoto N, Sakuma I, Asahina Y, Kurosaki M, Murakami T, Yamamoto C, et al: Mutations in the nonstructural protein 5A gene and response to interferon in patients with chronic hepatitis C virus 1b infection. N Engl J Med 1996;334:77–81.

5 Pascu M, Martus P, Hohne M, Wiedenmann B, Hopf U, Schreier E, et al: Sustained virological response in hepatitis C virus type 1b infected patients is predicted by the number of mutations within the NS5A-ISDR: a meta-analysis focused on geographical differences. Gut 2004;53:1345–1351.

6 Akuta N, Suzuki F, Sezaki H, Suzuki Y, Hosaka T, Someya T, et al: Association of amino acid substitution pattern in core protein of hepatitis C virus genotype 1b high viral load and non-virological response to interferon-ribavirin combination therapy. Intervirology 2005;48:372–380.

7 Donlin MJ, Cannon NA, Yao E, Li J, Wahed A, Taylor MW, et al: Pretreatment sequence diversity differences in the full-length hepatitis C virus open reading frame correlate with early response to therapy. J Virol 2007; 81:8211–8224.

8 Ge D, Fellay J, Thompson AJ, Simon JS, Shianna KV, Urban TJ, et al: Genetic variation in IL28B predicts hepatitis C treatment-induced viral clearance. Nature 2009;461:399–401.

9 Suppiah V, Moldovan M, Ahlenstiel G: *IL28B* is associated with response to chronic hepatitis C interferon-α and ribavirin therapy. Nat Genet 2009;41:1100–1104.

10 Tanaka Y, Nishida N, Sugiyama M, Kurosaki M, Matsuura K, Sakamoto N, et al: Genome-wide association of *IL28B* with response to pegylated interferon-α and ribavirin therapy for chronic hepatitis C. Nat Genet 2009; 41:1105–1109.

J Gastroenterol (2009) 44:1009–1015
DOI 10.1007/s00535-009-0126-7

REVIEW

# Viral factors influencing the response to the combination therapy of peginterferon plus ribavirin in chronic hepatitis C

**Shinya Maekawa · Nobuyuki Enomoto**

Received: 13 August 2009 / Accepted: 13 August 2009 / Published online: 11 September 2009


**Abstract** Hepatitis C virus (HCV) is a single-stranded RNA virus known for its high genetic variability owing to the lack of a proofreading mechanism of its RNA dependent RNA polymerase. Until now, numerous studies have been undertaken to clarify the correlation between pretreatment HCV genetic variability and the therapeutic response. Even with the recent combination therapy of peginterferon plus ribavirin for chronic hepatitis C, viral response is variable, and only half of treated patients could clear the virus [sustained viral response (SVR)]. In this review, the contribution of viral genetic variability affecting the treatment outcome is discussed according to each HCV genomic region.

**Keywords** Hepatitis C virus · Peginterferon plus ribavirin therapy · Viral predictive factor

## Introduction

Hepatitis C virus (HCV) is a major cause of chronic liver diseases worldwide; 180 million people, or some 3% of the world's population, are infected with HCV. Seventy percent of acute infections become persistent, and 50–75% of patients with chronic HCV infection progress to hepatocellular carcinoma. Though interferon-based therapy for HCV has been greatly advanced, half of patients still cannot eradicate the virus [sustained virological response (SVR)] even with the most recent combination therapy of peginterferon plus ribavirin [1].

HCV has a 9.5 kb single positive stranded RNA genome, and contains a single open reading frame flanked by 5′ and 3′ untranslated regions (UTR). HCV is classified as hepacivirus, a family of flaviridae. HCV is known for its high mutation rate owing to the lack of proofreading activity of its RNA dependent RNA polymerase ($1.4 \times 10^{-3}$ to $1.9 \times 10^{-3}$ substitutions/nucleotide/year [2, 3]). In accord with this mechanism, HCV presents a high degree of genetic variability, and the resultant molecular polymorphisms of HCV are suspected as one of the major causes determining the treatment responses.

## HCV genotypes

By phylogenetic analysis, HCV is classified into six major genotypes, and then further classified into subtypes in each genotype determined by their genetic distances [4]. Among all the viral factors investigated, viral genotypes are the most important, and a well-established predictive factor determining the treatment outcome. Geographically, genotypes 1–3 are associated with worldwide epidemic, while genotypes 4–6 are endemic. In comparison among major genotypes 1–3, a high SVR rate (~84%) was observed in patients with genotype 2 or 3, while a low SVR rate(~42%) was observed in genotype 1 [5–7]. Comparing between genotypes 2 and 3, genotype 2 could have more favorable outcomes [8, 9]. The study of genotype 4 was mainly from Egypt, and the SVR rate was reported to be intermediate (55–69%) [10, 11]. In genotypes 5 and 6, the SVR rate has been considered to be intermediate between the SVR of genotype 1 and genotypes 2–3, but studies

S. Maekawa · N. Enomoto (✉)
First Department of Internal Medicine, University of Yamanashi, 1110 Shimokato, Chuo, Yamanashi 409-3898, Japan
e-mail: enomoto@yamanashi.ac.jp

S. Maekawa
e-mail: maekawa@yamanashi.ac.jp

focusing on the response of genotype 5 and 6 are limited because of their minor distribution [12].

## Genomic regions and the treatment response

### 5′UTR

The 5′UTR of the HCV genome is 341 nucleotides long, and is the most conserved region throughout the HCV genome among different HCV genotypes. The 5′UTR together with the first 30 nucleotides of the core region acts as an internal ribosome entry site (IRES) regulating the cap-independent translation of HCV RNA to polyprotein. Secondary and tertiary conformation of IRES has the critical role in the initiation of polyprotein translation, and an IRES contains four highly structured domains (Domain I–IV). Since the structures play a pivotal role in HCV replication, changes in the conformation of an IRES, as well as changes in primary nucleotide sequence, result in a decrease of efficiency of protein translation. Therefore, it was suspected that IRES heterogeneity might correlate with the response to interferon-based therapy clinically. Several studies for interferon-based therapy, including peginterferon plus ribavirin, have been undertaken to date, however, its clinical value as a predictive factor for therapy is still in question, since most of these studies showed conflicting results of the relationship between 5′UTR variability and treatment response [13–18].

### Core

The core protein is considered to form the viral nucleocapsid of HCV, and its mature form consists of a secondary structure made of a large folded multimer of ~24 monomers. It is 21 kDa in size, and is separated into two domains, an N-terminal two-thirds hydrophilic domain (D1, residues 1–117) and a C-terminal one-third hydrophobic domain (D2, residues 118–170), respectively. The D1 domain contains many positively charged amino acids, and is implicated to bind RNA. The D2 domain is required for proper folding of domain D1. The mature core protein shares high homology among HCV genotypes. The core protein has been reported to interact with a variety of cellular proteins and to influence numerous host cell functions, such as its proapoptotic or antiapoptotic actions [19], immunomodulatory roles [20], or oxidative stress [21]. Recently, much attention has been paid to its relationships with liver steatosis, insulin resistance and hepatocellular carcinoma [22, 23]. HCV core proteins of genotype 3a and 1b were reported to interfere with the insulin signaling pathway in different ways depending on genotype-specific mechanisms [24].

As its contribution to the clinical treatment response, Akuta et al. first reported that substitutions of the amino acid 70 and 91 in the core protein were significantly related to the final outcome in the 48 weeks of interferon plus ribavirin combination therapy in 50 Japanese patients infected with genotype 1b HCV [25]. In successive studies, they reported that substitutions in those core regions were related to the final outcome, viral kinetics, early viral response, and extended 72 weeks of therapy [26–29]. They also reported substitution of core protein was associated with elevated alpha-fetoprotein, and hepatocarcinogenesis [29, 30]. Correlation of substitutions in the core protein in the treatment of interferon-based therapy was also reported in several other studies [31–33].

### E2

E2 is a type I transmembrane protein 70 kDa in size which assembles with E1 protein forming a heterodimer to become the mature viral envelope. It is a glycoprotein possessing several potential conserved glycosylation sites. Because the protein is essential for the virus's entry into hepatocytes, E2 interacts with potential HCV receptors, CD81, SR-BI [34] and occludin [35]. In E2, hypervariable region 1 (HVR1) was identified in the first 27 amino acids of the E2 ectodomain. HVR1 is known for its significant genomic variability and is suspected to be the target of antibodies. Its significant genetic variability could be induced by antibody selection.

#### *PePHD*

A region between amino acid residues of E2 659–670 is well-conserved, and is known as the phosphorylation site of PKR/eIF-2$\alpha$ phosphorylation homology domain (PePHD). The PePHD motif is similar to the phosphorylation sites of PKR and eIF2alpha. The PePHD has been shown to interact with PKR, one of the important antiviral proteins of the host cell, and inhibit antiviral action of PKR in vitro, suggesting a possible mechanism of HCV for countering the antiviral effects of interferon [36–38]. According to those observations, mutations in this PePHD were suspected to influence the clinical response to interferon-based therapy. However, the results of those studies are conflicting, and its clinical importance as the predictive value for treatment outcome has been controversial. Though some studies supported its significance [39–42], other recent studies could not find evident correlations [43–49].

### NS5A

NS5A is phosphorylated on multiple serine and threonine residues, and forms two distinct molecules of basal

phosphorylated form (p56) and hyperphosphorylated form (p58), being 56 and 58 kDa in size, respectively. The protein has three distinct domains (domains I, II, and III) being separated by low complexity sequences (LCS I and II). The study of the X-ray crystal structure analysis of domain I suggested that the NS5A is a dimer, and it forms a large putative RNA binding groove. Recent genetic study has shown many residues in domain II are essential for RNA replication, while domain III is less conserved and might be dispensable. Though the true function of NS5A is still under investigation, the protein is considered as a component of the HCV replication complex, where it modulates HCV replication through interaction with other viral proteins. Among all HCV proteins, NS5A has been most extensively explored for its relationship to interferon-based therapy.

*ISDR and PKR-BD*

The interferon sensitivity determining region (ISDR), located in the C-terminal half of NS5A, was originally identified as the 40 amino acid region (aa2209–2248) significantly related to the treatment outcome in the monotherapy of interferon-alpha in Japanese patients infected with genotype-1b HCV [50, 51]. The "mutant-type," having 4 or more mutations in the region, was associated with a high SVR rate (16/16: 100%), while the SVR rate was low in the "intermediate-type" [1–3 mutations: SVR rate 5/38 (13%)], or the "wild-type" [no mutation: SVR rate 30/30 (0%)]. Following studies from Japan were also concordant with the initial study [52–54]. However, controversy occurred as to the predictive value of ISDR since studies from Europe and North America did not necessarily report evident correlations between ISDR and treatment outcomes [55–60]. However, a recent meta-analysis study clearly confirmed its value, even in the Western countries [61]. Different results observed in North America and Europe might have been been caused partly by smaller rates of mutant-type patients in Western countries, and by the different treatment regimen in Japan compared to Western countries [62–66]. Though ISDR was found in the era of interferon monotherapy, its predictive value in the treatment outcome of the recent peginterferon plus ribavirin regimen has continued to be reported in most large cohort studies [26, 33, 67–69]. In searching for the biological ISDR function, Gale et al. reported that NS5A represses PKR through a direct interaction with the PKR binding domain (PKR-BD, aa2209–2274) and that the PKR-BD contains the ISDR [70]. Thus, they insisted that inactivation of PKR may be one mechanism by which HCV avoids the antiviral effects of interferon.

*V3 domain and IRRDR*

The V3 domain located in the C-terminal region of NS5A (aa2356–2379) was originally identified as a genomic region of genotype-1b HCV showing a marked heterogeneity between Japanese and American isolates [71]. A correlation of its mutations and the response to interferon-based therapy was first reported by Duverlie et al., and they reported that sequences of the V3 domain were highly conserved in resistant strains, but were highly variable in sensitive strains [72]. Most following studies also reported concordant results [46, 47, 68, 73, 74]. El-Shamy et al. reported a high degree of sequence variations in the V3 and the flanking pre-V3 regions (aa2334–2355) of NS5A, and they designated the region as the interferon/ribavirin resistance-determining region (IRRDR) (aa2334–2379). They reported that substitution number in the IRRDR was closely correlated with early virological response (EVR) by week 16 in 47 HCV-1b-infected patients treated with peginterferon plus ribavirin [75]. In their follow up study for the same group of patients, sequence variation in the IRRDR was also significantly related to the final outcome. The positive predictive values of IRRDR of 6 or more for SVR was 89% (16/18), whereas negative predictive values of IRRDR of 5 or less for non-SVR was 81% (22/27) [76].

*Other region in NS5A*

Pfeiffer et al. reported that two responsible mutations resided in the C-terminal region of NS5A: G404S and E442G were considered as mechanisms accounting for ribavirin resistance during HCV RNA replication, using HCV replicon-containing cell lines in the presence of increasing concentrations of ribavirin [77]. However, the clinical importance of such mutations and their relevance to ribavirin-related therapy is not evident.

NS5B

NS5B is 68 kDa proteins in size, and known as an RNA-dependent RNA polymerase. The enzyme synthesizes HCV–RNA using HCV–RNA as a template. NS5B is considered as one component of the HCV–RNA replication complex, and its activity as an RNA polymerase is modulated by NS3 and NS5A. Since this enzymatic activity is critical for HCV replication, the correlation between its mutations and treatment response has been explored, to date, in several studies.

Though the viral inhibitory mechanism of ribavirin in the treatment of HCV is unknown, its action as a mutagen is especially focused on the NS5B protein. During

ribavirin monotherapy, Young et al. reported that a specific mutation of NS5B amino acid 415 Phe-to-Tyr (F415Y) had emerged in five out of five patients infected with genotype-1a HCV [78]. To clarify the biological relevance of this mutation in ribavirin monotherapy, they introduced NS5B F415Y mutations into subgenomic HCV replicons, and reported that they observed different drug sensitivities in HCV replicons according to this NS5B polymorphism in a ribavirin dose-dependent manner. However, subsequent studies done in Japan and the UK could not find an evident relationship between specific selection of NS5B 415 mutations and the treatment of combination therapy of peginterferon and ribavirin. Sugihara et al. reported that they did not find specific mutations in NS5B 415 in the both serum obtained before and after therapy in 18 patients infected with genotype-1b HCV [79], and Ward et al. could not find evidence of a relationship of these mutations in the therapy of peginterferon and ribavirin in 15 patients infected with genotype-1a [80]. Hamano et al. explored genetic changes of genotype-1b HCV during the treatment of interferon-alpha and ribavirin, and reported that mutations at positions 300–358 of NS5B, including polymerase motif B–E, occurred more frequently in SVR patients or in end-of-treatment response patients when compared to null-response patients [81]. Mutation rate of NS5B in patients undergoing treatment with ribavirin monotherapy was also explored in patients treated with peginterferon/ribavirin therapy, since error catastrophe from an increase in mutation rate could be a possible mechanism of ribavirin in HCV infection [82]. Lutchman et al. reported that ribavirin was only associated with an early transient increase in the HCV mutation rate, but lethal mutagenesis and error catastrophe was unlikely to be the sole mechanism of ribavirin [83].

## Conclusions

Viral genetic variability of HCV and its potential correlation to the interferon-based treatment response is briefly discussed here. Understanding the biological features of drug-resistant HCV, may helpl us to predict the treatment response in each patient in advance. Furthermore, though trials of HCV specific protease inhibitors are on-going, and are just about to be incorporated into the new standard therapy, understanding those biological features of HCV would further clarify and focus which patients will most benefit from being treated with the new treatment regimens. This viral genetic approach could be crucial even in the era of HCV protease inhibitors for achieving global eradication of HCV.

## References


1. Zeuzem S. Interferon-based therapy for chronic hepatitis C: current and future perspectives. Nat Clin Pract Gastroenterol Hepatol. 2008;5(11):610–22.
2. Ogata N, Alter HJ, Miller RH, Purcell RH. Nucleotide sequence and mutation rate of the H strain of hepatitis C virus. Proc Natl Acad Sci USA. 1991;88(8):3392–6.
3. Okamoto H, Kojima M, Okada S, Yoshizawa H, Iizuka H, Tanaka T, et al. Genetic drift of hepatitis C virus during an 8.2-year infection in a chimpanzee: variability and stability. Virology. 1992;190(2):894–9.
4. Simmonds P, Bukh J, Combet C, Deleage G, Enomoto N, Feinstone S, et al. Consensus proposals for a unified system of nomenclature of hepatitis C virus genotypes. Hepatology. 2005;42(4):962–73.
5. Fried MW, Shiffman ML, Reddy KR, Smith C, Marinos G, Goncales FL Jr, et al. Peginterferon alfa-2a plus ribavirin for chronic hepatitis C virus infection. N Engl J Med. 2002;347(13):975–82.
6. Hadziyannis SJ, Sette H Jr, Morgan TR, Balan V, Diago M, Marcellin P, et al. Peginterferon-alpha2a and ribavirin combination therapy in chronic hepatitis C: a randomized study of treatment duration and ribavirin dose. Ann Intern Med. 2004;140(5):346–55.
7. Manns MP, McHutchison JG, Gordon SC, Rustgi VK, Shiffman M, Reindollar R, et al. Peginterferon alfa-2b plus ribavirin compared with interferon alfa-2b plus ribavirin for initial treatment of chronic hepatitis C: a randomised trial. Lancet. 2001;358(9286):958–65.
8. Dalgard O, Mangia A. Short-term therapy for patients with hepatitis C virus genotype 2 or 3 infection. Drugs. 2006;66(14):1807–15.
9. von Wagner M, Huber M, Berg T, Hinrichsen H, Rasenack J, Heintges T, et al. Peginterferon-alpha-2a (40 kDa) and ribavirin for 16 or 24 weeks in patients with genotype 2 or 3 chronic hepatitis C. Gastroenterology. 2005;129(2):522–7.
10. El-Zayadi AR, Attia M, Barakat EM, Badran HM, Hamdy H, El-Tawil A, et al. Response of hepatitis C genotype-4 naive patients to 24 weeks of Peg-interferon-alpha2b/ribavirin or induction-dose interferon-alpha2b/ribavirin/amantadine: a non-randomized controlled study. Am J Gastroenterol. 2005;100(11):2447–52.
11. Kamal SM, El Tawil AA, Nakano T, He Q, Rasenack J, Hakam SA, et al. Peginterferon {alpha}-2b and ribavirin therapy in chronic hepatitis C genotype 4: impact of treatment duration and viral kinetics on sustained virological response. Gut. 2005;54(6):858–66.
12. Nguyen MH, Keeffe EB. Prevalence and treatment of hepatitis C virus genotypes 4, 5, and 6. Clin Gastroenterol Hepatol. 2005;3(10 Suppl 2):S97–101.
13. Araujo FM, Sonoda IV, Rodrigues NB, Teixeira R, Redondo RA, Oliveira GC. Genetic variability in the 5' UTR and NS5A regions of hepatitis C virus RNA isolated from non-responding and responding patients with chronic HCV genotype 1 infection. Mem Inst Oswaldo Cruz. 2008;103(6):611–4.
14. El Awady MK, Azzazy HM, Fahmy AM, Shawky SM, Badreldin NG, Yossef SS, et al. Positional effect of mutations in 5'UTR of hepatitis C virus 4a on patients' response to therapy. World J Gastroenterol. 2009;15(12):1480–6.
15. Katano Y, Hayashi K, Ishigami M, Itoh A, Hirooka Y, Nakano I, et al. Association with 5'-untranslated region and response to interferon in chronic hepatitis C. Hepatogastroenterology. 2007;54(75):854–7.
16. Soler M, Pellerin M, Malnou CE, Dhumeaux D, Kean KM, Pawlotsky JM. Quasi species heterogeneity and constraints on the

evolution of the 5′ noncoding region of hepatitis C virus (HCV): relationship with HCV resistance to interferon-alpha therapy. Virology. 2002;298(1):160–73.
17. Thelu MA, Drouet E, Hilleret MN, Zarski JP. Lack of clinical significance of variability in the internal ribosome entry site of hepatitis C virus. J Med Virol. 2004;72(3):396–405.
18. Yamamoto C, Enomoto N, Kurosaki M, Yu SH, Tazawa J, Izumi N, et al. Nucleotide sequence variations in the internal ribosome entry site of hepatitis C virus-1b: no association with efficacy of interferon therapy or serum HCV-RNA levels. Hepatology. 1997;26(6):1616–20.
19. Kountouras J, Zavos C, Chatzopoulos D. Apoptosis in hepatitis C. J Viral Hepat. 2003;10(5):335–42.
20. Hahn YS. Subversion of immune responses by hepatitis C virus: immunomodulatory strategies beyond evasion? Curr Opin Immunol. 2003;15(4):443–9.
21. Wang T, Weinman SA. Causes and consequences of mitochondrial reactive oxygen species generation in hepatitis C. J Gastroenterol Hepatol. 2006;21(Suppl 3):S34–7.
22. Mori Y, Moriishi K, Matsuura Y. Hepatitis C virus core protein: its coordinate roles with PA28gamma in metabolic abnormality and carcinogenicity in the liver. Int J Biochem Cell Biol. 2008;40(8):1437–42.
23. Serfaty L, Capeau J. Hepatitis C, insulin resistance and diabetes: clinical and pathogenic data. Liver Int. 2009;29(Suppl 2):13–25.
24. Pazienza V, Clement S, Pugnale P, Conzelman S, Foti M, Mangia A, et al. The hepatitis C virus core protein of genotypes 3a and 1b downregulates insulin receptor substrate 1 through genotype-specific mechanisms. Hepatology. 2007;45(5):1164–71.
25. Akuta N, Suzuki F, Sezaki H, Suzuki Y, Hosaka T, Someya T, et al. Association of amino acid substitution pattern in core protein of hepatitis C virus genotype 1b high viral load and non-virological response to interferon–ribavirin combination therapy. Intervirology. 2005;48(6):372–80.
26. Akuta N, Suzuki F, Hirakawa M, Kawamura Y, Yatsuji H, Sezaki H, et al. A matched case-controlled study of 48 and 72 weeks of peginterferon plus ribavirin combination therapy in patients infected with HCV genotype 1b in Japan: amino acid substitutions in HCV core region as predictor of sustained virological response. J Med Virol. 2009;81(3):452–8.
27. Akuta N, Suzuki F, Kawamura Y, Yatsuji H, Sezaki H, Suzuki Y, et al. Predictors of viral kinetics to peginterferon plus ribavirin combination therapy in Japanese patients infected with hepatitis C virus genotype 1b. J Med Virol. 2007;79(11):1686–95.
28. Akuta N, Suzuki F, Kawamura Y, Yatsuji H, Sezaki H, Suzuki Y, et al. Predictive factors of early and sustained responses to peginterferon plus ribavirin combination therapy in Japanese patients infected with hepatitis C virus genotype 1b: amino acid substitutions in the core region and low-density lipoprotein cholesterol levels. J Hepatol. 2007;46(3):403–10.
29. Akuta N, Suzuki F, Kawamura Y, Yatsuji H, Sezaki H, Suzuki Y, et al. Amino acid substitutions in the hepatitis C virus core region are the important predictor of hepatocarcinogenesis. Hepatology. 2007;46(5):1357–64.
30. Akuta N, Suzuki F, Kawamura Y, Yatsuji H, Sezaki H, Suzuki Y, et al. Substitution of amino acid 70 in the hepatitis C virus core region of genotype 1b is an important predictor of elevated alpha-fetoprotein in patients without hepatocellular carcinoma. J Med Virol. 2008;80(8):1354–62.
31. Donlin MJ, Cannon NA, Yao E, Li J, Wahed A, Taylor MW, et al. Pretreatment sequence diversity differences in the full-length hepatitis C virus open reading frame correlate with early response to therapy. J Virol. 2007;81(15):8211–24.
32. Mori N, Imamura M, Kawakami Y, Saneto H, Kawaoka T, Takaki S, et al. Randomized trial of high-dose interferon-alpha-2b combined with ribavirin in patients with chronic hepatitis C: Correlation between amino acid substitutions in the core/NS5A region and virological response to interferon therapy. J Med Virol. 2009;81(4):640–9.
33. Okanoue T, Itoh Y, Hashimoto H, Yasui K, Minami M, Takehara T, et al. Predictive values of amino acid sequences of the core and NS5A regions in antiviral therapy for hepatitis C: a Japanese multi-center study. J Gastroenterol. 2009;11 [Epub ahead of print].
34. Grove J, Nielsen S, Zhong J, Bassendine MF, Drummer HE, Balfe P, et al. Identification of a residue in hepatitis C virus E2 glycoprotein that determines scavenger receptor BI and CD81 receptor dependency and sensitivity to neutralizing antibodies. J Virol. 2008;82(24):12020–9.
35. Benedicto I, Molina-Jimenez F, Barreiro O, Maldonado-Rodriguez A, Prieto J, Moreno-Otero R, et al. Hepatitis C virus envelope components alter localization of hepatocyte tight junction-associated proteins and promote occludin retention in the endoplasmic reticulum. Hepatology. 2008;48(4):1044–53.
36. Pavio N, Taylor DR, Lai MM. Detection of a novel unglycosylated form of hepatitis C virus E2 envelope protein that is located in the cytosol and interacts with PKR. J Virol. 2002;76(3):1265–72.
37. Taylor DR, Shi ST, Romano PR, Barber GN, Lai MM. Inhibition of the interferon-inducible protein kinase PKR by HCV E2 protein. Science. 1999;285(5424):107–10.
38. Taylor DR, Tian B, Romano PR, Hinnebusch AG, Lai MM, Mathews MB. Hepatitis C virus envelope protein E2 does not inhibit PKR by simple competition with autophosphorylation sites in the RNA-binding domain. J Virol. 2001;75(3):1265–73.
39. Gupta R, Subramani M, Khaja MN, Madhavi C, Roy S, Habibullah CM, et al. Analysis of mutations within the 5′ untranslated region, interferon sensitivity region, and PePHD region as a function of response to interferon therapy in hepatitis C virus-infected patients in India. J Clin Microbiol. 2006;44(3):709–15.
40. Saito T, Ito T, Ishiko H, Yonaha M, Morikawa K, Miyokawa A, et al. Sequence analysis of PePHD within HCV E2 region and correlation with resistance of interferon therapy in Japanese patients infected with HCV genotypes 2a and 2b. Am J Gastroenterol. 2003;98(6):1377–83.
41. Sarrazin C, Bruckner M, Herrmann E, Ruster B, Bruch K, Roth WK, et al. Quasi species heterogeneity of the carboxy-terminal part of the E2 gene including the PePHD and sensitivity of hepatitis C virus 1b isolates to antiviral therapy. Virology. 2001;289(1):150–63.
42. Sarrazin C, Kornetzky I, Ruster B, Lee JH, Kronenberger B, Bruch K, et al. Mutations within the E2 and NS5A protein in patients infected with hepatitis C virus type 3a and correlation with treatment response. Hepatology. 2000;31(6):1360–70.
43. Gaudy C, Lambele M, Moreau A, Veillon P, Lunel F, Goudeau A. Mutations within the hepatitis C virus genotype 1b E2-PePHD domain do not correlate with treatment outcome. J Clin Microbiol. 2005;43(2):750–4.
44. Hung CH, Lee CM, Lu SN, Lee JF, Wang JH, Tung HD, et al. Mutations in the NS5A and E2-PePHD region of hepatitis C virus type 1b and correlation with the response to combination therapy with interferon and ribavirin. J Viral Hepat. 2003;10(2):87–94.
45. Munoz de Rueda P, Casado J, Paton R, Quintero D, Palacios A, Gila A, et al. Mutations in E2-PePHD, NS5A-PKRBD, NS5A-ISDR, and NS5A-V3 of hepatitis C virus genotype 1 and their relationships to pegylated interferon-ribavirin treatment responses. J Virol. 2008;82(13):6644–53.
46. Murphy MD, Rosen HR, Marousek GI, Chou S. Analysis of sequence configurations of the ISDR, PKR-binding domain, and V3 region as predictors of response to induction interferon-alpha and ribavirin therapy in chronic hepatitis C infection. Dig Dis Sci. 2002;47(6):1195–205.

47. Vuillermoz I, Khattab E, Sablon E, Ottevaere I, Durantel D, Vieux C, et al. Genetic variability of hepatitis C virus in chronically infected patients with viral breakthrough during interferon–ribavirin therapy. J Med Virol. 2004;74(1):41–53.
48. Yang SS, Lai MY, Chen DS, Chen GH, Kao JH. Mutations in the NS5A and E2-PePHD regions of hepatitis C virus genotype 1b and response to combination therapy of interferon plus ribavirin. Liver Int. 2003;23(6):426–33.
49. Yoon J, Lee JI, Baik SK, Lee KH, Sohn JH, Lee HW, et al. Predictive factors for interferon and ribavirin combination therapy in patients with chronic hepatitis C. World J Gastroenterol. 2007;13(46):6236–42.
50. Enomoto N, Sakuma I, Asahina Y, Kurosaki M, Murakami T, Yamamoto C, et al. Comparison of full-length sequences of interferon-sensitive and resistant hepatitis C virus 1b. Sensitivity to interferon is conferred by amino acid substitutions in the NS5A region. J Clin Invest. 1995;96(1):224–30.
51. Enomoto N, Sakuma I, Asahina Y, Kurosaki M, Murakami T, Yamamoto C, et al. Mutations in the nonstructural protein 5A gene and response to interferon in patients with chronic hepatitis C virus 1b infection. N Engl J Med. 1996;334(2):77–81.
52. Chayama K, Tsubota A, Kobayashi M, Okamoto K, Hashimoto M, Miyano Y, et al. Pretreatment virus load and multiple amino acid substitutions in the interferon sensitivity-determining region predict the outcome of interferon treatment in patients with chronic genotype 1b hepatitis C virus infection. Hepatology. 1997;25(3):745–9.
53. Komatsu H, Fujisawa T, Inui A, Miyagawa Y, Onoue M. Mutations in the nonstructural protein 5A gene and response to interferon therapy in young patients with chronic hepatitis C virus 1b infection. J Med Virol. 1997;53(4):361–5.
54. Kurosaki M, Enomoto N, Murakami T, Sakuma I, Asahina Y, Yamamoto C, et al. Analysis of genotypes and amino acid residues 2209–2248 of the NS5A region of hepatitis C virus in relation to the response to interferon-beta therapy. Hepatology. 1997;25(3):750–3.
55. Chung RT, Monto A, Dienstag JL, Kaplan LM. Mutations in the NS5A region do not predict interferon-responsiveness in American patients infected with genotype 1b hepatitis C virus. J Med Virol. 1999;58(4):353–8.
56. Hofgartner WT, Polyak SJ, Sullivan DG, Carithers RL Jr, Gretch DR. Mutations in the NS5A gene of hepatitis C virus in North American patients infected with HCV genotype 1a or 1b. J Med Virol. 1997;53(2):118–26.
57. Khorsi H, Castelain S, Wyseur A, Izopet J, Canva V, Rombout A, et al. Mutations of hepatitis C virus 1b NS5A 2209–2248 amino acid sequence do not predict the response to recombinant interferon-alfa therapy in French patients. J Hepatol. 1997;27(1):72–7.
58. Odeberg J, Yun Z, Sonnerborg A, Weiland O, Lundeberg J. Variation in the hepatitis C virus NS5a region in relation to hypervariable region 1 heterogeneity during interferon treatment. J Med Virol. 1998;56(1):33–8.
59. Squadrito G, Leone F, Sartori M, Nalpas B, Berthelot P, Raimondo G, et al. Mutations in the nonstructural 5A region of hepatitis C virus and response of chronic hepatitis C to interferon alfa. Gastroenterology. 1997;113(2):567–72.
60. Zeuzem S, Lee JH, Roth WK. Mutations in the nonstructural 5A gene of European hepatitis C virus isolates and response to interferon alpha. Hepatology. 1997;25(3):740–4.
61. Pascu M, Martus P, Hohne M, Wiedenmann B, Hopf U, Schreier E, et al. Sustained virological response in hepatitis C virus type 1b infected patients is predicted by the number of mutations within the NS5A-ISDR: a meta-analysis focused on geographical differences. Gut. 2004;53(9):1345–51.
62. Pawlotsky JM, Germanidis G, Neumann AU, Pellerin M, Frainais PO, Dhumeaux D. Interferon resistance of hepatitis C virus genotype 1b: relationship to nonstructural 5A gene quasi species mutations. J Virol. 1998;72(4):2795–805.
63. Saiz JC, Lopez-Labrador FX, Ampurdanes S, Dopazo J, Forns X, Sanchez-Tapias JM, et al. The prognostic relevance of the nonstructural 5A gene interferon sensitivity determining region is different in infections with genotype 1b and 3a isolates of hepatitis C virus. J Infect Dis. 1998;177(4):839–47.
64. Sarrazin C, Berg T, Lee JH, Ruster B, Kronenberger B, Roth WK, et al. Mutations in the protein kinase-binding domain of the NS5A protein in patients infected with hepatitis C virus type 1a are associated with treatment response. J Infect Dis. 2000; 181(2):432–41.
65. Sarrazin C, Berg T, Lee JH, Teuber G, Dietrich CF, Roth WK, et al. Improved correlation between multiple mutations within the NS5A region and virological response in European patients chronically infected with hepatitis C virus type 1b undergoing combination therapy. J Hepatol. 1999;30(6):1004–13.
66. Witherell GW, Beineke P. Statistical analysis of combined substitutions in nonstructural 5A region of hepatitis C virus and interferon response. J Med Virol. 2001;63(1):8–16.
67. Shirakawa H, Matsumoto A, Joshita S, Komatsu M, Tanaka N, Umemura T, et al. Pretreatment prediction of virological response to peginterferon plus ribavirin therapy in chronic hepatitis C patients using viral and host factors. Hepatology. 2008; 48(6):1753–60.
68. Veillon P, Payan C, Le Guillou-Guillemette H, Gaudy C, Lunel F. Quasi species evolution in NS5A region of hepatitis C virus genotype 1b during interferon or combined interferon–ribavirin therapy. World J Gastroenterol. 2007;13(8):1195–203.
69. Yen YH, Hung CH, Hu TH, Chen CH, Wu CM, Wang JH, et al. Mutations in the interferon sensitivity-determining region (nonstructural 5A amino acid 2209–2248) in patients with hepatitis C-1b infection and correlating response to combined therapy of pegylated interferon and ribavirin. Aliment Pharmacol Ther. 2008;27(1):72–9.
70. Gale MJ Jr, Korth MJ, Tang NM, Tan SL, Hopkins DA, Dever TE, et al. Evidence that hepatitis C virus resistance to interferon is mediated through repression of the PKR protein kinase by the nonstructural 5A protein. Virology. 1997;230(2):217–27.
71. Inchauspe G, Zebedee S, Lee DH, Sugitani M, Nasoff M, Prince AM. Genomic structure of the human prototype strain H of hepatitis C virus: comparison with American and Japanese isolates. Proc Natl Acad Sci USA. 1991;88(22):10292–6.
72. Duverlie G, Khorsi H, Castelain S, Jaillon O, Izopet J, Lunel F, et al. Sequence analysis of the NS5A protein of European hepatitis C virus 1b isolates and relation to interferon sensitivity. J Gen Virol. 1998;79(Pt 6):1373–81.
73. Puig-Basagoiti F, Forns X, Furcic I, Ampurdanes S, Gimenez-Barcons M, Franco S, et al. Dynamics of hepatitis C virus NS5A quasi species during interferon and ribavirin therapy in responder and non-responder patients with genotype 1b chronic hepatitis C. J Gen Virol. 2005;86(Pt 4):1067–75.
74. Sarrazin C, Herrmann E, Bruch K, Zeuzem S. Hepatitis C virus nonstructural 5A protein and interferon resistance: a new model for testing the reliability of mutational analyses. J Virol. 2002;76(21):11079–90.
75. El-Shamy A, Sasayama M, Nagano-Fujii M, Sasase N, Imoto S, Kim SR, et al. Prediction of efficient virological response to pegylated interferon/ribavirin combination therapy by NS5A sequences of hepatitis C virus and anti-NS5A antibodies in pretreatment sera. Microbiol Immunol. 2007;51(4):471–82.
76. El-Shamy A, Nagano-Fujii M, Sasase N, Imoto S, Kim SR, Hotta H. Sequence variation in hepatitis C virus nonstructural protein 5A predicts clinical outcome of pegylated interferon/ribavirin combination therapy. Hepatology. 2008;48(1):38–47.

77. Pfeiffer JK, Kirkegaard K. Ribavirin resistance in hepatitis C virus replicon-containing cell lines conferred by changes in the cell line or mutations in the replicon RNA. J Virol. 2005;79(4):2346–55.
78. Young KC, Lindsay KL, Lee KJ, Liu WC, He JW, Milstein SL, et al. Identification of a ribavirin-resistant NS5B mutation of hepatitis C virus during ribavirin monotherapy. Hepatology. 2003;38(4):869–78.
79. Sugihara K, Orito E, Tanaka Y, Kato T, Lau JY, Ohno T, et al. Variations in the viral NS5B region in Japanese patients with chronic hepatitis C virus genotype 1b infection. No specific amino acid substitution was identified as determinants of treatment response to interferon/ribavirin combination therapy. Intervirology. 2006;49(6):319–26.
80. Ward CL, Dev A, Rigby S, Symonds WT, Patel K, Zekry A, et al. Interferon and ribavirin therapy does not select for resistance mutations in hepatitis C virus polymerase. J Viral Hepat. 2008 [Epub ahead of print].
81. Hamano K, Sakamoto N, Enomoto N, Izumi N, Asahina Y, Kurosaki M, et al. Mutations in the NS5B region of the hepatitis C virus genome correlate with clinical outcomes of interferon-alpha plus ribavirin combination therapy. J Gastroenterol Hepatol. 2005;20(9):1401–9.
82. Asahina Y, Izumi N, Enomoto N, Uchihara M, Kurosaki M, Onuki Y, et al. Mutagenic effects of ribavirin and response to interferon/ribavirin combination therapy in chronic hepatitis C. J Hepatol. 2005;43(4):623–9.
83. Lutchman G, Danehower S, Song BC, Liang TJ, Hoofnagle JH, Thomson M, et al. Mutation rate of the hepatitis C virus NS5B in patients undergoing treatment with ribavirin monotherapy. Gastroenterology. 2007;132(5):1757–66.

BioSystems 99 (2010) 70–78

Contents lists available at ScienceDirect

BioSystems

journal homepage: www.elsevier.com/locate/biosystems

# Reproducibility and usability of chronic virus infection model using agent-based simulation; comparing with a mathematical model

Jun Itakura[a,*], Masayuki Kurosaki[a], Yoshie Itakura[a], Sinya Maekawa[b], Yasuhiro Asahina[a], Namiki Izumi[a], Nobuyuki Enomoto[b]

[a] Division of Gastroenterology and Hepatology, Musashino Red Cross Hospital, 1-26-1 Kyonan-cho, Musashino-shi, Tokyo 180-8610, Japan
[b] First Department of Internal Medicine, Faculty of Medicine, University of Yamanashi, 1110, Shimogatou, Chuou-shi, Yamanashi 409-3898, Japan

ARTICLE INFO

*Article history:*
Received 30 June 2009
Received in revised form 27 August 2009
Accepted 6 September 2009

*Keywords:*
Agent-based model
Virus infectious disease

ABSTRACT

We created agent-based models that visually simulate conditions of chronic viral infections using two software. The results from two models were consistent, when they have same parameters during the actual simulation. The simulation results comprise a transient phase and an equilibrium phase, and unlike the mathematical model, virus count transit smoothly to the equilibrium phase without overshooting which correlates with actual biology in vivo of certain viruses. We investigated the effects caused by varying all the parameters included in concept; increasing virus lifespan, uninfected cell lifespan, uninfected cell regeneration rate, virus production count from infected cells, and infection rate had positive effects to the virus count during the equilibrium period, whereas increasing the latent period, the lifespan-shortening ratio for infected cells, and the cell cycle speed had negative effects. Virus count at the start did not influence the equilibrium conditions, but it influenced the infection development rate. The space size had no intrinsic effect on the equilibrium period, but virus count maximized when the virus moving speed was twice the space size. These agent-based simulation models reproducibly provide a visual representation of the disease, and enable a simulation that encompasses parameters those are difficult to account for in a mathematical model.



## 1. Introduction

All viruses need hosts as a basis for their life. When a virus enters the host body, it invades cells and uses both its own enzymes and those of the host cells to replicate. Host cells infected by viruses launch a self-defense system known as the innate immune system (See and Wark, 2008; Naniche, 2009), which inhibits viral replication and uses the human leukocyte antigen system and cytokines to elicit an immune response. Immune cells that have received signals from host cells activate other immune cells, neutralize viruses in the serum by means of antibodies, and prevent the virus from replicating and proliferating by destroying or curing host cells. Viral infection is a disorder based on the interactions between viruses and cells.

The power relationship between these agents changes along with the progression of the disease. In the very early stages of infection, as the host defense mechanisms are immature, the virus has the ability to overwhelm the host cells, actively replicate, and proliferate. Subsequently, as the capacity of the immune system improves, the speed of viral proliferation drops and the virus count reaches a peak. Infected host cells begin to be disrupted by the immune system or virus particles, and symptoms appear as a result. If the immune system is stronger than the virus, then the viral counts decline, and, in transient viral disorders, the virus is finally eliminated and the host recovers. In chronic viral disorders, however, the power relationship between the virus and host cells reaches equilibrium, and a long-term power balance is maintained with the virus count reaching a plateau.

Mathematical models have been proposed to study the dynamics of such viral disorders, and are regarded as being of value in understanding this phenomenon (Ho et al., 1995; Nowak et al., 1996; Neumann et al., 1998). However, these models are difficult to understand for clinicians, and their applicability is somewhat limited in everyday practice. In clinical research, measurements of viral dynamics in patients for short duration have been made for human

*Abbreviations:* HIV, human immunodeficiency virus; HBV, hepatitis B virus; HCV, hepatitis C virus.

* Corresponding author. Tel.: +81 422 32 3111; fax: +81 422 32 9551.
*E-mail address:* jitakura@musashino.jrc.or.jp (J. Itakura).

0303-2647/$ – see front matter © 2009 Elsevier Ireland Ltd. All rights reserved.
doi:10.1016/j.biosystems.2009.09.001

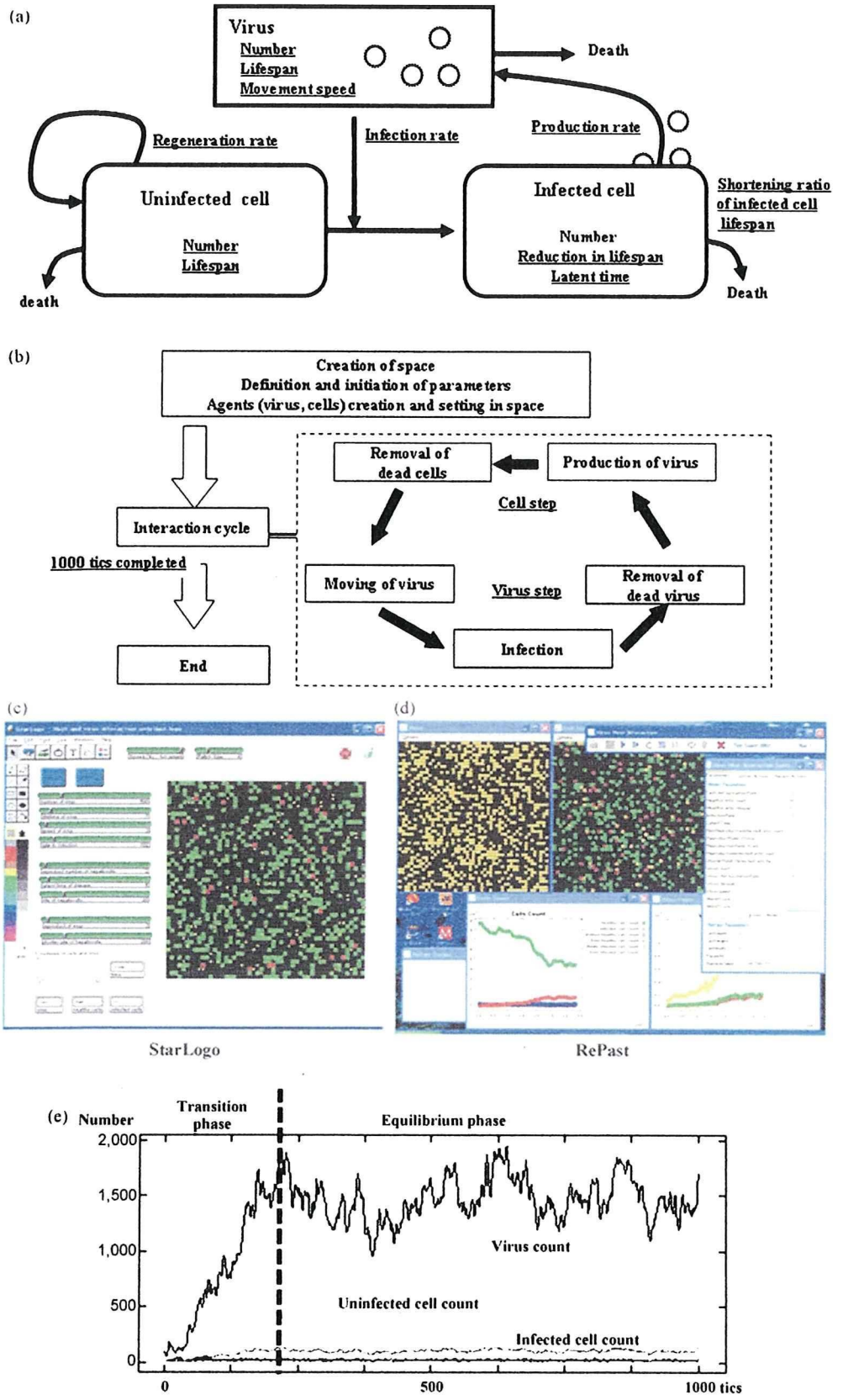


**Fig. 1.** Simulation design and an example of simulation results. (a) Model concept. Viruses, uninfected cells, and infected cells were treated as agents, and parameters were set for each of these and for interactions between agents (underlined). (b) Flowchart of the program. After preparing the simulation, we entered the interaction cycle, in which virus steps (such as movement) and cell steps were repeated. One cycle was counted as 1 tic, and the simulation concluded after 1000 tics. (c and d) Simulation screen using (c) StarLogo and (d) RePast. Yellow circles are viruses, green squares are uninfected cells, and orange and red indicate infected cells, with orange indicating the latent period. In StarLogo, all the agents are shown on the same screen, but in RePast, viruses and cells are shown in separate windows. (e) Example of a simulation chart in StarLogo. After the start of simulation the virus count and infected cell count increase while the uninfected cell count decreases, with equilibrium state reached after a certain number of tics.

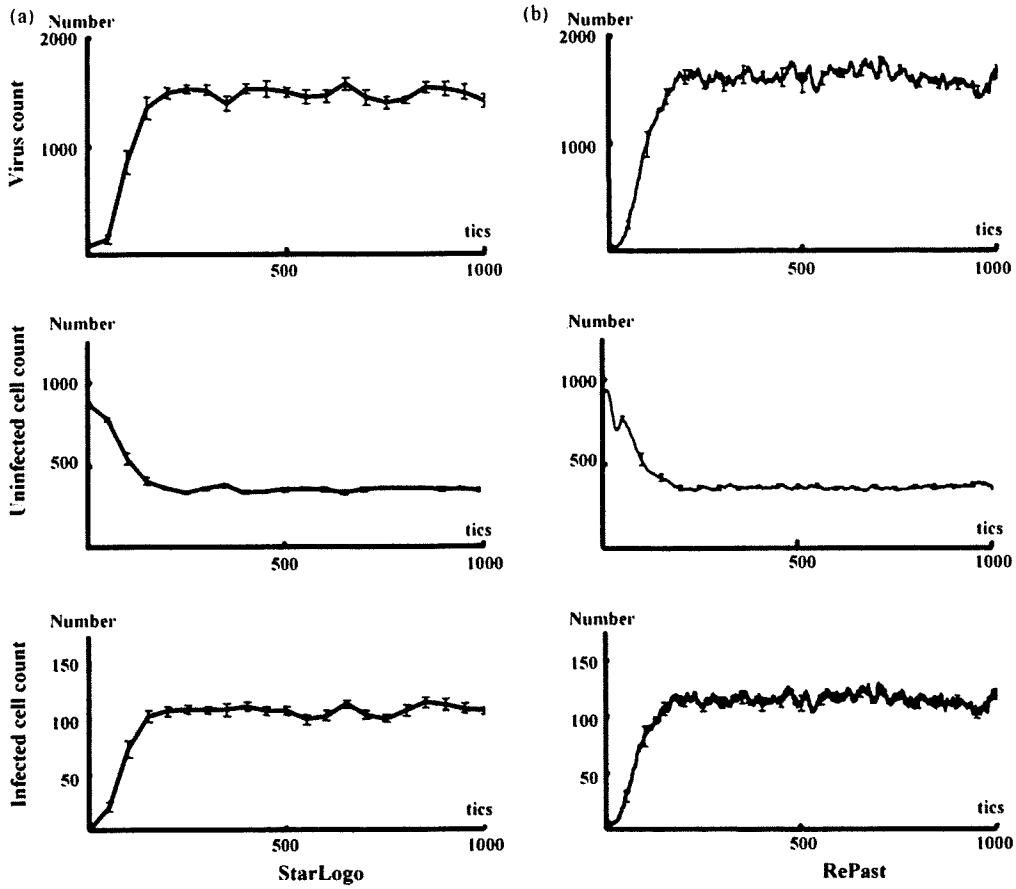


**Fig. 2.** Comparison of simulation results in (a) StarLogo and (b) RePast. The results were consistent when the parameters were made consistent. (Virus count [average ± SD]: StarLogo 1458.03 ± 173.1, RePast 1462.71 ± 178.8, $p = 0.94$. Uninfected cell count: 364.24 ± 30.4, 368.11 ± 33.4, $p = 0.83$. Infected cell count: 105.73 ± 13.0, 107.74 ± 13.0, $p = 0.24$. Unpaired Student's $t$-test.) Parameter values were set as follows: initial virus count, 100; uninfected cell count, 880; infected cell count, 0; virus speed of movement, 5 grids/tic; infection rate, 10%; uninfected cell regeneration rate, 1%; latent period, 3 tics; and virus reproduction rate, 5/cells/tic. The following parameter settings were taken from actual measurements: virus lifespan, 4.5 tics; uninfected cell lifespan, 49.8 tics; and infected cell lifespan, 6.7 tics.

immunodeficiency virus (HIV) (Ho et al., 1995), hepatitis B virus (HBV) (Nowak et al., 1996) and hepatitis C virus (HCV) (Neumann et al., 1998), and research is also underway on a range of models based on animal experiments and cell culture systems. As chronic viral disorders persist over long periods of time complete follow-up of viral dynamics is difficult. Furthermore, limitations of items that can be measured, such as the difficulty of measuring whole numbers of host cells, make it extremely difficult to investigate their consistency in mathematical models.

The recent ascend of dynamic-models owes much to advances in computers. Computer performance has improved markedly in recent years, not only in terms of their calculating capacity but also with regard to image displays, and models that offer a visual representation of viral disorders are now being reported (Gilbert and Bankes, 2002; Duca et al., 2007; Shapiro et al., 2008; Castiglione et al., 2007). One advantage of such visual models is that by providing a visual representation, they make understanding the disease status easy. Another benefit is that they enable parameters to be identified that are hidden as background noise in mathematical models. However, these models have some problems; it is difficult to prove the reproducibility of the simulation results derived from different languages or libraries, difficult to prove the validity of the model's concepts, and difficult to prove that the simulation results accurately reflect the reality. In this study, we created agent-based computer models that visually simulate the conditions of chronic viral infections using two software. The reproducibility of two agent-based computer models and the differences between agent-based models and the mathematical model were analyzed. This agent-based model enabled us to investigate how each parameter included in the concept affects the conditions of chronic viral infections.

## 2. Methods

### 2.1. Selection of Software

In this study, we used two different types of softwares: StarLogo version 2.0 (http://education.mit.edu/starlogo/) supplied by MIT Media Laboratory and Recursive Porous Agent Simulation Toolkit (RePast-3.0, http://repast.sourceforge.net/) supplied by the Argonne National Laboratory. StarLogo uses Logo, one of the simplest programming languages, and has a fixed graphical user interface. RePast is a library that uses Java, another programming language, which also has a fixed graphical user interface.

Logo is an assembly language, and StarLogo carries out processing sequentially. Java is an object-oriented language, and RePast has a faster processing speed than StarLogo. In addition, StarLogo has a number of stipulations to simplify simulations, such as parameters can only be set up to five decimal places and the simulation space is also fixed as 51 × 51 square grids. RePast, on the other hand, has fewer such restrictions. Thus, it offers a higher degree of freedom in program settings than StarLogo. Taking simulation space as an example, in spite of the restrictions imposed by the underlying operating system's image display system, any number of grids can be set and a hexagonal grid could also be chosen rather than a square one. However, users must stipulate and set all parameters themselves. This means that they must first declare the shape of the grid and the number of grids they will use to fill the simulation space. Java is also more difficult to learn than Logo, and debugging and correcting the program is also more difficult. Thus, it is difficult to judge whether or not the results agree with the planned simulation.

In effect, these two different types of softwares are polar opposites. It is simple to start a simulation in StarLogo, but producing results takes time and it is difficult to carry out more complex simulations. In RePast it is difficult to compose the program and judge whether or not the planned study has actually been achieved, but the

simulation itself takes only a short time to complete and there are lesser restrictions in the construction of a simulation model.

### 2.2. Concept for Modeling

We applied the basic virus–host interaction mathematical model to the agent-based simulation system with slight modifications. The mathematical model was used to describe the dynamics of HIV (Ho et al., 1995), HBV (Nowak et al., 1996), and HCV (Neumann et al., 1998) and the only agents involved were host cells and viruses, without the inclusion of immune cells. The effects of the immune system are expressed by varying parameters such as lifespan of host cells and viruses.

Fig. 1a illustrates the study concept. Viruses have the ability to infect healthy host cells (uninfected cells) and the infected cells produce new viruses. Both cells and viruses have definite lifespans, and the lifespan of infected cells is usually shorter than that of uninfected cells. Uninfected cells automatically regenerate within the space, whereas infected cells only arise due to infection of uninfected cells. Viruses also lack the ability to regenerate themselves and are only produced from infected cells.

### 2.3. Parameter Settings

In the present study, as the StarLogo settings are circumscribed, we limited the simulation space to 51 × 51 square grids. However, we made an exception here while investigating the effects of size of space on the simulation results. The numbers of viruses, uninfected cells, and infected cells could only be set before the start of the simulation. As described in the later, our simulation ran in cycles, with 1 cycle defined as 1 tic.

In mathematical simulation models, the death rate is required as a parameter. However, in our program we set lifespans for viruses and uninfected cells. These lifespans were not uniform, but were set to have a deviation of about 10%. The lifespan of cells was shortened by infection with ratio decided beforehand.

The infection ratio was meaningful only when an infected cell and a virus coincidentally occupied the same grid, and this was used to calculate the probability of the infection occurring in that situation. The virus production rate was set as the number of viruses produced by an infected cell during 1 tic. Infected cells could be set as a parameter indicating the latent period between the time of virus infection and the time of virus replication.

In order to emulate the tissue repair capacity, we set uninfected cell regeneration rate such that grids without any cells had a specified probability of producing uninfected cells on top of themselves. As a result, the more the cell count declined within a space the more regenerated uninfected cells were produced, whereas the number of regenerated cells declined as cell count increased.

The number of grids through which a virus could move in 1 tic was set as the speed of movement, and the direction of movement was set within a range of 90° toward the top of the simulation space. The program used a circulatory method of movement; when a virus arrived at the top of the space, it was translocated to the bottom, and moved again toward the top. Cells were fixed on the grid.

### 2.4. Simulation Flowchart

Fig. 1b shows a flowchart of the program. First, the simulation space was produced, after which each parameter was defined and the initial settings were made. Next the agents – viruses and uninfected and infected cells – were produced. The simulation cycle was as follows. Viruses moved to a new grid, and if an uninfected cell was present, this was infected with a probability based on the infection rate. The lifespan of the virus decreased, and viruses that had completed their lifespan and those that had caused an infection were removed from the space. Infected cells produced new viruses, the lifespans of both uninfected and infected cells decreased. Then, cells that had completed their lifespan were eliminated and a new cycle began. The program was set such that the simulation ended after this cycle had repeated 1000 times. This meant that one simulation was complete after 1000 tics.

### 2.5. Data Collection

The RePast model was programmed such that data for each tic was saved automatically as a text file at the end of the simulation. This text file could be opened by a database software. The StarLogo model was programmed to stop the simulation and collect data after every 50 tics.

### 2.6. Mathematical Model

In order to compare the results of this agent-based simulation, we used a viral infection mathematical model, which we improved as follows.

$$\frac{dT}{dt} = s[2601 - (T + I)] - dT - bVT \quad (1)$$

$$\frac{dI}{dt} = bVT - dI \quad (2)$$

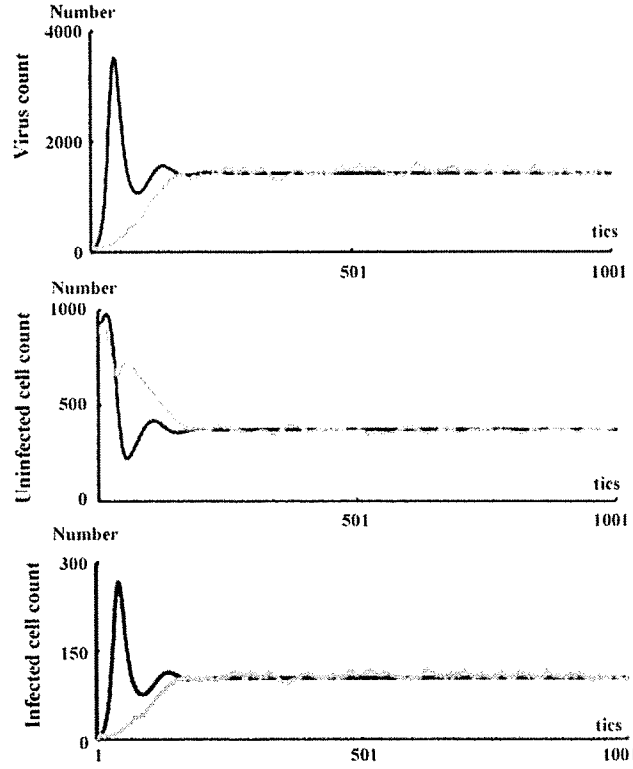


**Fig. 3.** Comparison of results of agent-based simulation and mathematical simulation. Both sets of results were consistent for the equilibrium phase, but differed in the shift in transition phase. Black line: mathematical model; grey line: results of simulation in RePast. Parameter values were set as follows: initial virus count, 100; uninfected cell count, 880; infected cell count, 0; virus speed of movement, 5 grids/tic; infection rate, 10%; uninfected cell regeneration rate, 1%; latent period, 3 tics; virus reproduction rate, 5/cells/tic; virus lifespan, 10 tics; uninfected cell lifespan, 50 tics; and cell lifespan-shortening ratio as a result of infection, 69%.

$$\frac{dV}{dt} = pI - cV \quad (3)$$

where, $T$ is the uninfected cell count, $I$ is the infected cell count, and $V$ is the virus count. Uninfected cells are supplied to the space with a probability $s[2601 - (T+I)]$, as the number of grids in this agent-based simulation model was 2601 ($51 \times 51$). The death rate of uninfected cells is $d$, the death rate of infected cells is $\delta$, and the death rate of viruses is $c$. The infection rate is indicated by $\beta$. Viruses are released from infected cells at a probability $p$.

### 2.7. Statistical Analysis

Statistical analyses were performed by statistical tests using the program StatView 5.0 (SAS Institute Inc.). All tests of significance were two-tailed, with $p$ values of $<0.05$ considered to be significant.

## 3. Results

### 3.1. Reproducibility of Chronic Viral Infection Disease Models Using Agent-based Simulation Methods

We constructed the chronic viral infection model with StarLogo library. Fig. 1c shows the simulation screen, and Fig. 1e shows one sample result. Immediately after the start of the simulation, the virus count temporarily dropped in accordance with the onset of an infection. Subsequently, the virus count started to increase with an increase in the infected cells and a decrease in the uninfected cells. After a certain number of tics (around 300 in this example), although the virus count, infected cell count, and uninfected cell count had some fluctuation, an equilibrium state was reached. We use the following descriptive terms in this paper: the transient phase is the period during which virus growth peaks, and the equilibrium phase is the period during which an equilibrium state is

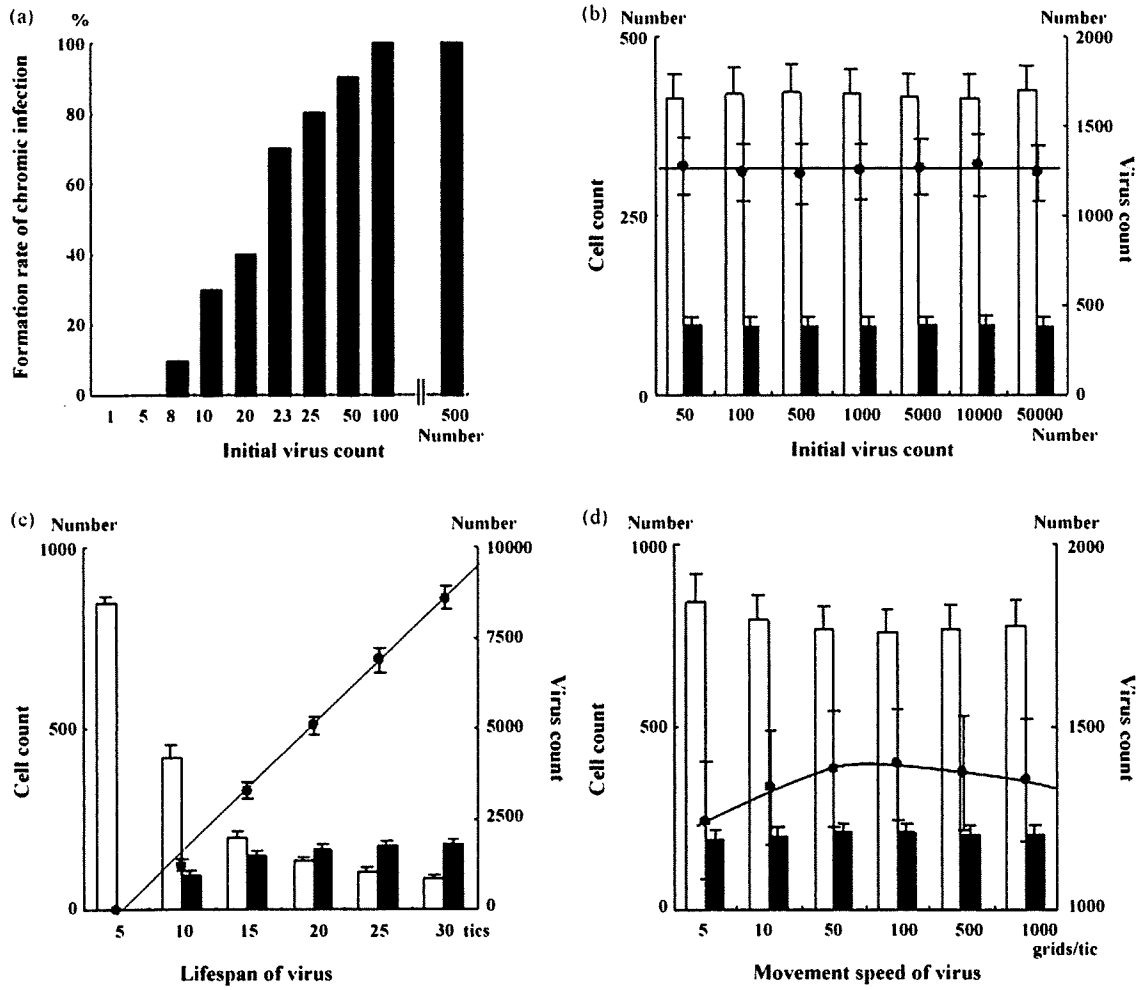


**Fig. 4.** Effects of changes in viral parameters. (a) The higher the initial virus count, the greater is the increase in the rate of formation of chronic infection, but (b) there was no effect on the conditions in the equilibrium phase. (c) Extending the virus lifespan increased the virus count. (d) Increasing the speed of virus movement to 100 grids/tic increased the virus count, but increasing it to 500 grids/tic had the opposite effect, with a slight declining trend. (a) Black bars: number of infections produced; (b–d) black circles: virus count; line: virus count approximation curve; white bars: uninfected cell count; black bars: infected cell count.

established. When the simulation was performed multiple times, the features described above were maintained, and the average values for virus, infected cell, and uninfected cell counts during the equilibrium state were all consistent.

Fig. 1d shows the simulation screen of the RePast. When we attempted setting all the initial parameters to the same values as those in the StarLogo, the results were not consistent. When we recalculated the parameters from the simulation results, in RePast, the parameters were largely maintained at the levels of the settings, but in StarLogo, the lifespans of both cell types became shorter than the settings while the simulation was in progress. We made the results of both simulations consistent by using the same parameters during the actual simulation (Fig. 2a and b).

### 3.2. Comparison Between Agent-based Simulation Models and Mathematical Simulation Model

We investigated whether the results of a chronic viral infection disease model produced by RePast would be consistent with the results of a mathematical model. For the mathematical model, we carried out an approximate integration using a four-dimensional Runge–Kutta method to ensure that the uninfected cell count and infected cell count would be in the same class. Parameters were always fixed as constant between simulations. The simulation results were consistent for the equilibrium phase, but transitions in virus count during the transient phase varied, with a shift to equilibrium state following two overshoots in the mathematical model, but a monotonic increase following a logistic curve in the agent-based model (Fig. 3). In the mathematical model, when the equilibrium condition was calculated with $dT/dt = dI/dt = dV/dt = 0$, the equilibrium-phase virus count, uninfected cell count, and infected cell count were very similar to those of the agent-based model (virus count: mathematical model 371.8/space, agent-based model 371.1 ± 32.4/space [average ± SD]; uninfected cell count: mathematical model 1605/space, agent-based model 1454 ± 194/space; infected cell count: mathematical model 115.9/space, agent-based model 108.3 ± 14.2/space).

### 3.3. Usability of the Models; Effect of Changing Parameters

We investigated the changes in the equilibrium phase brought about by changing each parameter. All the investigations below were carried out by using RePast, and we used the average values from ten simulations.

### 3.4. Viral Parameters

The lower the virus counts at the beginning of the simulation, the lower the probability of a chronic infection (Fig. 4a). However, the initial virus count did not have any effect on the equilibrium

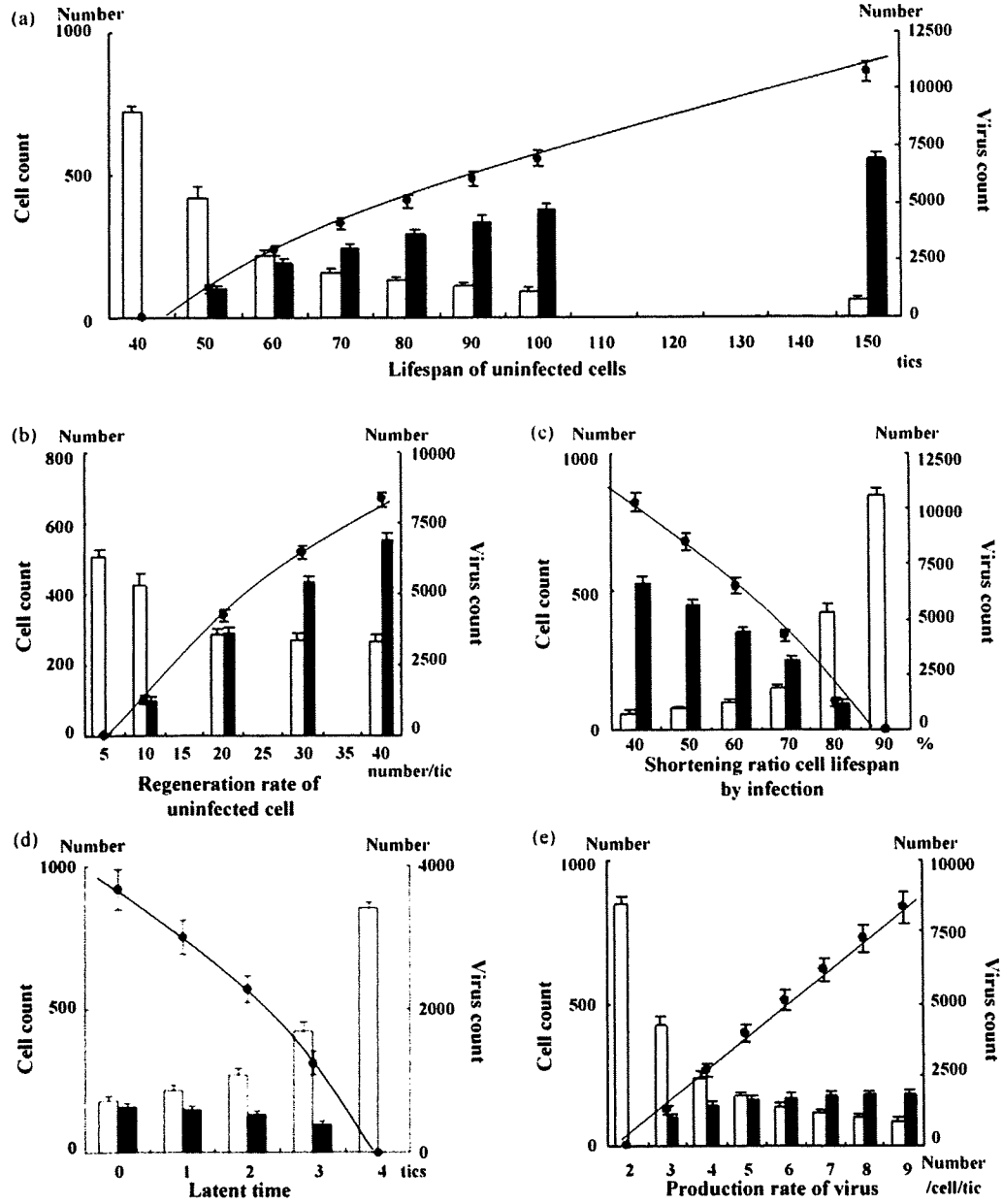


**Fig. 5.** Effects of changes in cell parameters. (a) Extending the uninfected cell lifespan and (b) increasing the uninfected cell regeneration rate increased the virus count. (c) Raising the lifespan-shortening ratio as a result of infection shortened the lifespan of infected cells, thereby decreasing the virus count. (d) Extending the latent period shortened the period of virus production from infected cells, thereby decreasing the virus count. (e) Increasing the virus production count resulted in a linear increase in equilibrium-phase virus count. Black circles: virus count; line: virus count approximation curve; white bars: uninfected cell count; black bars: infected cell count.

phase itself (Fig. 4b). Extending the lifespan of viruses resulted in a linear increase in equilibrium-phase virus count (Fig. 4c). Although the infected cell count increased, the rate of increase gradually declined. Changing the speed of viral movement resulted in the equilibrium-phase virus count to eventually decline after 100 grids/tic was reached, allowing movement over an area twice the size of the simulation space (Fig. 4d).

### 3.5. Uninfected Cell Parameters

Extending the lifespan of uninfected cells led to an increased virus count during the equilibrium phase (Fig. 5a). Increasing the uninfected cell regeneration rate also contributed to increased equilibrium-phase virus count (Fig. 5b). In both the cases, the increases in virus count and infected cell count were not linear, but showed a tendency for the rate of increase to decline gradually.

### 3.6. Infected Cell Parameters

We carried out an investigation of the effects of variation in the lifespan-shortening ratio on the virus count on the assumption that cell lifespan is shortened by infection. When this ratio was increased, the virus count decreased (Fig. 5c). An extended latent period was also related to a decreased virus count (Fig. 5d). However, the virus production from infected cells led to a linear increase in the virus count (Fig. 5e).

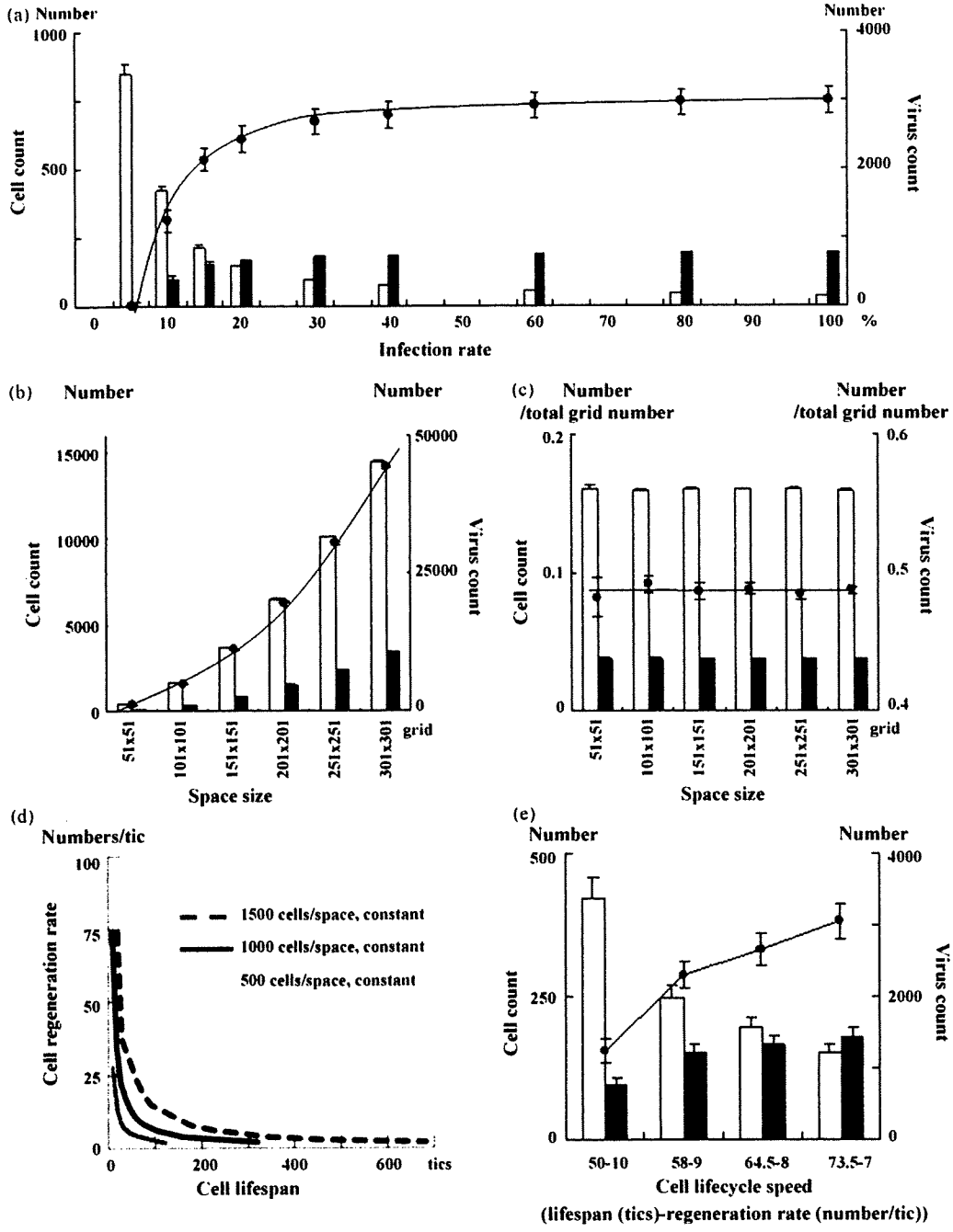


**Fig. 6.** (a) Increasing the infection rate increased the virus count in equilibrium periods, but the virus count did not change at infection rates of 30% or more. (b) The size of the simulation space increased not only virus count but also the cell count; however, (c) when virus and cell counts were divided by the total number of grids in the space, they were constant for all space sizes. (d) Changing the lifespan and regeneration rate of uninfected cells in opposite directions at the same time makes it possible to change only the cell cycle speed without altering the uninfected cell count. (e) When the cell cycle speed was reduced, the virus count increased toward the right of the graph. This may be because the effect of extending the lifespan of cells exceeds that of reducing their regeneration rate. (a–c and e) Black circles: virus count; line: virus count approximation curve; white bars: uninfected cell count; black bars: infected cell count.

### 3.7. Infection Rate and Space Size

Increasing the infection rate caused an increase in the virus count, but the change was minimal at an infection rate of 30% or more. The same results were seen for infected cell count, but a decrease in uninfected cell count resulted in a tendency for the infection rate to decrease by up to 60% (Fig. 6a).

The larger the space, higher the increase in both virus and cell counts (Fig. 6b). This increase was proportional to space size, however, when virus and cell counts were divided by the total number of grids in the space they were all constant (Fig. 6c).

### 3.8. Cell Cycle Speeds

Running a simulation with the initial virus count set to zero enables only the equilibrium condition for uninfected cells to be simulated. Changing the lifespan and regeneration rate of uninfected cells in opposite directions at the same time makes it possible

to change the cell cycle speed without altering the uninfected cell count (Fig. 6d). We used this technique to investigate how changing the cell cycle speed affected the equilibrium phase. Fig. 6e shows the results. Cell lifespan increases while the cell cycle speed declines. The equilibrium virus count increased in accordance with slower cell cycle speeds.

## 4. Discussion

In this study, we investigated the models using two agent-based simulation methods to program a simple virus–host chronic infection model. The same model written in two different programming language systems displayed the same results. The transient phase was unlike that seen in a mathematical simulation with no overshoot in virus count, but rather a smooth transition to the equilibrium phase. The virus count at the start of the simulation only had effect on the rate of infection development. Increases in virus lifespan, uninfected cell lifespan, uninfected cell regeneration rate, virus production count from infected cells, and infection rate all led to increased equilibrium-phase virus count. Rises in the infected cell lifespan-shortening ratio, latent period, and cell cycle speed decreased the equilibrium-phase virus count. The size of the space itself had no innate effect on the equilibrium phase, but a speed of movement of the virus that was twice the size of the space produced the maximum virus count.

Reproducibility is the basis for all scientific study, but there are many problems to prove it in computer simulations, such as programming bugs. As agent-based simulation deals with numerous agents individually, it requires vast amounts of calculations. Accumulation of very small change of values leads to large differences of results. In this study, we investigated two programs based on two programming languages to confirm the reproducibility of our simulation results in different programming languages. The results of two simulations were consistent, but in StarLogo, the lifespan parameters had a tendency to be lower than when they were set while simulations were actually in progress. This may be because the number of digits used in calculations was different between the two programs. RePast performs calculations to at least eight decimal places. In StarLogo, the library settings only enable settings to be made up to five decimal places. It is probable that these small differences accumulate during repeated calculations and are reflected in the simulation. Ultimately, we confirmed that the differences in results obtained by using different libraries and programming languages were not innate and by making the parameters consistent during simulation, consistent results were obtained.

Mathematical models using formulae for HIV therapy was published in 1994, the method has since been applied to HBV and HCV (Ho et al., 1995; Nowak et al., 1996; Neumann et al., 1998), and they were thought to be good reflections of the reality. In the mathematical model, viruses and cells are conceived as individuals in the concept itself, but both of them are perceived *en masse* when calculations are performed. However a feature of the agent-based simulation is that it deals with individual viruses and cells as separate agents. By moving each agent individually, it probes the factors influencing overall shifts from the micro viewpoint. When the space is viewed as a whole, it is possible to watch on the screen the collective movement of groups of agents. Recently, models that provide a visual representation of Epstein-Barr virus and HIV infection have been reported, both of which are useful for an instinctive and intuitive understanding (Duca et al., 2007; Shapiro et al., 2008; Castiglione et al., 2007).

In agent-based simulation model, virus count transit smoothly to the equilibrium phase. On the other hand, virus counts overshoot during transient phase in mathematical model. We think this difference is derived from technicality of different modeling. The difference in concepts between mathematical models and agent-based models is the space. The mathematical model has no space in concept, but agents move across the space in the agent-based model. In agent-based models, the densities of virus and cells change overtime especially in the transition phase because of the limited space. These changes of the densities of virus and cells lead to the dynamic change of the encounter rate of viruses and cells. The mathematical model does not make such concept of the density; the encounter rate is constant. This may be the reason for the difference between two models in the transition phase. Since no overshoot of virus counts in transient phase had been reported from in vivo studies of hepatitis C virus and simian immunodeficiency virus (Dahari et al., 2005; Nowak et al., 1997), agent-based model correlates with actual biology in vivo at least for these viruses. The increase of initial virus count at the start of simulation correlates with higher encounter rate of viruses and cells which make the linear increasing of infection forming rate. Mathematical model can only express the infection formation rate as "infected or not".

The importance of viral passing speed in the agent-based model is also explained by the "space". Although the virus actually moves through the blood stream in our body and virus could not decide their moving speeds by themselves, there is most appropriate speed for virus to meet the cells on the simulation space by the highest probability. The effect of cell cycle speed should be mentioned by another affection of the space. A fast cell cycle speed means that the lifespan of uninfected cells is short. Then fast cell cycle speed leads to the short lifespan of infected cells. A higher regeneration rate for uninfected cells results in a higher rate of infection among uninfected cells by viruses, but in situations where viruses and cells are dispersed around the space this is ineffective in increasing the infection rate, as the latter depends on the probability that they will encounter one another. As a result, the infected cell count decreases during the equilibrium phase, as does the virus count.

In this study, we confirmed the reproducibility and usability of agent-based models in expressing the interaction between viruses and cells. A feature of this simulation system is that it uses the concept of space as actual space, which means that the existence of the space becomes an additional controlling factor on the simulation results. This is a concept that is absent from mathematical models. The reality is that we have a spatial existence, and an advantage of the agent-based simulation system is the fact that it accounts for the space. Another feature of the simulation system is that it enables the condition to be perceived in visual terms, making it easy to understand. However it may be affected by computer performance and by the limitations of programming languages or the program itself, this system may offer a powerful tool for the future analysis of real virus–host interaction disease.

## Conflict of interest

No conflicts of interest exist for all authors.

## References

Castiglione, F., Pappalardo, F., Bernaschi, M., Motta, S., 2007. Optimization of HAART with genetic algorithms and agent-based models of HIV infection. Bioinformatics 23, 3350–3355, doi:10.1093/bioinformatics/btm408.

Dahari, H., Major, M., Zhang, X., Mihalik, K., Rice, C.M., Perelson, A.S., Feinstone, S.M., Neumann, A.U., 2005. Mathematical modeling of primary hepatitis c infection: noncytolytic clearance and early blockage of virion production. Gastroenterology 128, 1056–1066, doi:10.1053/j.gastro.2005.01.049.

Duca, K.A., Shapiro, M., Delgado-Eckert, E., Hadinoto, V., Jarrah, A.S., Laubenbacher, R., Lee, K., Luzuriaga, K., Polys, N.F., Thorley-Lawson, D.A., 2007. A virtual look at Epstein-Barr virus infection: biological interpretations. PLoS Pathog. 3, 1388–1400, doi:10.1371/journal.ppat.0030137.

Gilbert, N., Bankes, S., 2002. Platforms and methods for agent-based modelling. Proc. Natl. Acad. Sci. U.S.A. 99 (Suppl. 3), 7197–7198.

Ho, D.D., Neumann, A.U., Perelson, A.S., Chen, W., Leonard, J.M., Markowitz, M., 1995. Rapid turnover of plasma virions and CD4 lymphocytes in HIV-1 infection. Nature 373, 123–126, doi:10.1038/373123a0.

Naniche, D., 2009. Human immunology of measles virus infection. Curr. Top. Microbiol. Immunol. 330, 151–171.

Neumann, A.U., Lam, N.P., Dahari, H., Gretch, D.R., Wiley, T.E., Layden, T.J., Perelson, A.S., 1998. Hepatitis C viral dynamics in vivo and the antiviral efficacy of interferon-alpha therapy. Science 282, 103–107, doi:10.1126/science.282.5386.103.

Nowak, M.A., Bonhoeffer, S., Hill, A.M., Boehme, R., Thomas, H.C., McDade, H., 1996. Viral dynamics in hepatitis B virus infection. Proc. Natl. Acad. Sci. U.S.A. 93, 4398–4402.

Nowak, M.A., Lloyd, A.L., Vasquez, G.M., Wiltrout, T.A., Wahl, L.M., Biscofberger, N., Williams, J., Kinter, A., Fauci, A.S., Hirsch, V.M., Lifson, J.D., 1997. Viral dynamics of primary viremia and antiretroviral therapy in simian immunodeficiency virus infection. J. Virol. 71, 7518–7525.

Shapiro, M., Duca, K.A., Lee, K., Delgado-Eckert, E., Hawkins, J., Jarrah, A.S., Laubenbacher, R., Polys, N.F., Hadinoto, V., Thorley-Lawson, D.A., 2008. A virtual look at Epstein-Barr virus infection: simulation mechanism. J. Theor. Biol. 252, 633–648, doi:10.1016/j.jtbi.2008.01.032.

See, H., Wark, P., 2008. Innate immune response to viral infection of the lungs. Paediatr. Respir. Rev. 9, 243–250, doi:10.1016/j.prrv.2008.04.001.

*Hepatology Research* 2009; 39: 60–69 doi: 10.1111/j.1872-034X.2008.00398.x

***Original Article***

# Two flavonoids extracts from *Glycyrrhizae radix* inhibit *in vitro* hepatitis C virus replication

Yuko Sekine-Osajima,[1]* Naoya Sakamoto,[1,2]* Mina Nakagawa,[1,2] Yasuhiro Itsui,[1] Megumi Tasaka,[1] Yuki Nishimura-Sakurai,[1] Cheng-Hsin Chen,[1] Goki Suda,[1] Kako Mishima,[1] Yuko Onuki,[1] Machi Yamamoto,[1] Shinya Maekawa,[3] Nobuyuki Enomoto,[3] Takanori Kanai,[1] Kiichiro Tsuchiya,[1] and Mamoru Watanabe[1]

*Department of [1]Gastroenterology and Hepatology and [2]Department for Hepatitis Control, Tokyo Medical and Dental University, Tokyo, and [3]First Department of Internal Medicine, University of Yamanashi, Yamanashi, Japan*

*Aim:* Traditional herbal medicines have been used for several thousand years in China and other Asian countries. In this study we screened herbal drugs and their purified compounds, using the Feo replicon system, to determine their effects on *in vitro* HCV replication.

*Methods:* We screened herbal drugs and their purified extracts for the activities to suppress hepatitis C virus (HCV) replication using an HCV replicon system that expressed chimeric firefly luciferase reporter and neomycin phosphotransferase (Feo) genes. We tested extracts and 13 purified compounds from the following herbs: *Glycyrrhizae radix*; *Rehmanniae radix*; *Paeoniae radix*; *Artemisiae capillari spica*; and *Rhei rhizoma*.

*Results:* The HCV replication was significantly and dose-dependently suppressed by two purified compounds, isoliquiritigenin and glycycoumarin, which were from *Glycyrrhizae radix*. Dose-effect analyses showed that 50% effective concentrations were 6.2 ± 1.0 μg/mL and 15.5 ± 0.8 μg/mL for isoliquiritigenin and glycycoumarin, respectively. The MTS assay did not show any effect on cell growth and viability at these effective concentrations, indicating that the effects of the two compounds were specific to HCV replication. These two compounds did not affect the HCV IRES-dependent translation nor did they show synergistic action with interferon-alpha.

*Conclusion:* Two purified herbal extracts, isoliquiritigenin and glycycoumarin, specifically suppressed *in vitro* HCV replication. Further elucidation of their mechanisms of action and evaluation of *in vivo* effects and safety might constitute a new anti-HCV therapeutics.

**Key words:** hepatitis C virus, herbal drugs, replicon

## INTRODUCTION

HEPATITIS C VIRUS (HCV) infects 170 million people worldwide and is characterized by chronic liver inflammation and fibrogenesis leading to end-stage liver failure and hepatocellular malignancy.[1,2] The difficulty in eradicating HCV is attributable, in part, to limited treatment options against the virus. Currently, combination therapy using pegylated interferon-alpha (IFN) and ribavirin has been used worldwide.[3–5] The success rates, however, are almost half of patients treated. Furthermore, these therapies carry a significant risk of serious side effects. Thus, the development of alternative therapeutic agents against HCV is our high priority goal.

We have reported an HCV subgenomic replicon that expresses chimeric luciferase reporter "Feo" protein.[6] This Feo replicon supports stable and high levels of autonomous HCV RNA replication in transfected cells. Furthermore, the level of luciferase correlates well with levels of HCV RNA production, so that luciferase can be used as a reliable surrogate marker for HCV replication. This chimeric reporter replicon system has contributed the discovery of novel anti-HCV substances such as cyclosporins,[7–9] short interfering RNA,[10,11] interferon-gamma[12] and HMG-CoA reductase inhibitors.[13,14]

Traditional herbal drugs have been used for several thousand years in China and other Asian countries. Although these pharmacological activities are not fully

*Correspondence: Dr Naoya Sakamoto, Department of Gastroenterology and Hepatology, Tokyo Medical and Dental University, 1-5-45 Yushima, Bunkyo-ku, Tokyo 113-8519, Japan. Email: nsakamoto.gast@tmd.ac.jp*
*Y.S. and N.S. contributed equally to this work.
*Received 30 September 2007; revised 28 February 2008; accepted 16 May 2008.*

**Table 1** List of herbal drugs and their purified extracts

| Herbal drug | Purified compound |
|---|---|
| *Glycyrrhizae radix* | Isoliquiritigenin |
| | Glycycoumarin |
| | Isoliquiritin |
| | Licuroside |
| *Paeoniae radix* | Paeoniflorin |
| | 1,2,3,6-tetra-O-galloyl-β-D-glucose |
| *Rhei Rhizoma* | Rhein 8-O-β-glucoside |
| *Rehmanniae radix* | Acteoside |
| | Martynoside |
| | Isoacteoside |
| *Artemisiae capillari spica* | Demethoxycapillarisin |
| | 3,4-di-o-galloylquinic acid |
| | Acteosyringone |

characterized, they also have been safely used for many clinical conditions in Japan. For example, Sho-saiko-to (TJ-9; Xiao-Chae-Hu-Tang in Chinese), an oral medicine, which consists of seven herbal components (*Bupleuri radix, Pinelliae tuber, Scutellariae radix, Ginseng radix, Grycyrrhhizae radix, and Zingiberis rhizoma*),[15] has been clinically used for the treatment of chronic viral liver disease. It has been reported to regulate the cytokine production system in patients with hepatitis C[16] and to prevent the development of HCC in patients with non-B cirrhosis.[17] *Glycyrrhizin*, the major component of *Glycyrrhizae radix* (licorice), has also been used for the treatment of chronic hepatitis in Japan, known to have an alanine transaminase-lowering effect.[18,19] Despite the clinical effects of these herbal drugs, they did not suppress the HCV replication *in vitro*.[15]

In the present study, we applied the Feo replicon system to screen the herbal drugs and their purified compounds for their effects on *in vitro* HCV replication. Here, we show that two purified compounds from the herbal extracts specifically and substantially suppressed HCV replication.

## MATERIALS AND METHODS

### Purified compounds (Table 1)

THIRTEEN COMPOUNDS WERE purified from five herbal drugs: *Glycyrrhizae radaix; Rhemanniae radix; Paeoniae radix; Artemisiae Capillari Spica;* and *Rhei Rhizoma* (Table 1; Tsumura, Tokyo, Japan). These extracts were prepared at concentrations of 5 mg/mL in dimethyl sulfoxide (DMSO), then stored at −20°C until use. Recombinant human interferon (IFN) alpha-2b was obtained from Schering-Plough (NJ, USA).

### Cell culture

A human hepatoma cell line, Huh7, was maintained in Dulbecco's modified Eagle's medium (Sigma, MO, USA) supplemented with 10% fetal calf serum at 37°C under 5% $CO_2$. Huh7 cells expressing the HCV replicon were cultured in a medium containing 200 μg/mL G418 (Wako, Osaka, Japan).

### HCV subgenomic replicon construct

An HCV subgenomic replicon plasmid, pHCV1bneo-delS,[20] was reconstructed by substituting the neomycin phosphotransferase gene with a fusion gene comprising the firefly luciferase and neomycin phosphotrasnferase (pRep-Feo) (Fig. 1a). RNA was synthesized from pRep-

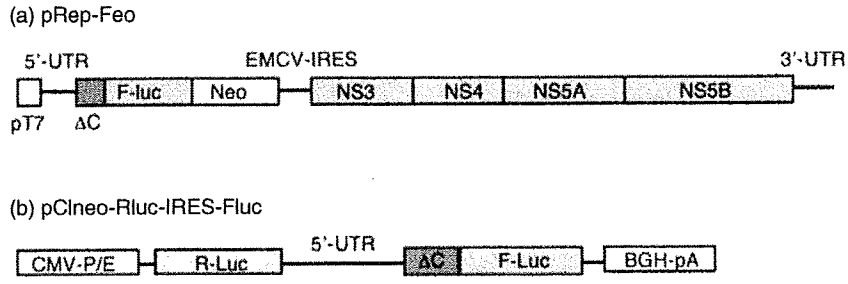


**Figure 1** HCV subgenomic replicon and reporter plasmid constructs. (a) An HCV subgenomic replicon plasmid, pRep-Feo, was reconstructed from HCV1bneo-delS by replacing the neomycin phosphotransferase (Neo) gene with a fusion gene comprising the firefly luciferase (Fluc) and Neo, which we designated as "Feo"[6]. NS, nonstructural region; pT7, T7 promoter; 3' UTR, 3' untranslated region. (b) A plasmid, pCIneo-Rluc-IRES-Fluc, was constructed to analyze HCV-IRES-mediated translation efficiency. The plasmid, expressing a bicistronic RNA, in which *Renilla* luciferase (Rluc) was translated in a cap-dependent manner and firefly luciferase (Fluc) was translated by HCV-internal ribosome entry site (IRES)-mediated initiation, was stably transfected into Huh7 cells.

Feo and transfected into Huh7 cells. After culture in the presence of G418, cell lines stably expressing the replicon were established.[10,21]

## HCV-IRES reporter construct

A plasmid, pCIneo-Rluc-IRES-Fluc, was used to analyze HCV internal ribosome entry site (IRES)-mediated translation efficiency (Fig. 1b).[22] The plasmid, expressing a bicistronic RNA, in which *Renilla* luciferase (Rluc) was translated in a cap-dependent manner and firefly luciferase (Fluc) was translated by HCV-IRES-mediated initiation, was stably transfected into Huh7 cells. After culture in the presence of G418, Huh7/CRIF cells were established.[9] Activities of the HCV-IRES-mediated translation were measured by culture of Huh7/CRIF cells in the presence of drugs and by dual luciferase assays after 48 h.

## Luciferase assays and measurements of antiviral activity

Huh7/Rep-Feo cells were cultured with various concentrations of herbal extracts or compounds. Levels of HCV replication were quantified by internal luciferase assay after 48 h of culture. Luciferase activities were quantified using a luminometer (Promega, WI, USA) and the Bright-Glo Luciferase Assay System (Promega). Assays were performed in triplicate and the results were expressed as means ± SD as percentages of the controls. The 50% effective concentrations (EC50) were calculated using probit method. The determination of EC50 was performed three times, and presented as mean ± SD in each compound.

## Realtime RT-PCR analysis

Total cellular RNA was extracted from cultured cells or liver tissue using ISOGEN (Nippon Gene, Tokyo, Japan). Two μg of total cellular RNA was used to generate cDNA from each sample using the SuperScript II reverse-transcriptase (Invitrogen, CA, USA). The replicon RNA expression levels were measured using the Applied Biosystems 7500 Fast Realtime PCR System (Applied Biosystems, CA, USA) and QuantiTect SYBR Green PCR Kit (QIAGEN, CA, USA). Sequences of a pair of primers has been described elsewhere.[23]

## Northern blottings

Expression of HCV subgenomic RNA was detected as previously reported.[24] Total cellular RNA was extracted from cells using ISOGEN (Nippon Gene, Tokyo, Japan). Fifteen micrograms of the total cellular RNA was electrophoresed on a 1.0% denaturing agarose-formaldehyde gel and was transferred to a Hybond-N+ nylon membrane (Amersham-Pharmacia Biotech, Sweden). The upper part of the membrane, which contained the HCV replicon RNA, was hybridized with a digoxigenin-labeled probe that was specific for the full-length replicon sequence, and the lower part of the membrane was hybridized with a probe specific for beta-actin. The signals were detected in a chemiluminescence reaction using a Digoxigenin Luminescent Detection Kit (Roche, Germany) and visualized using a Fluoro-Imager (Roche).

## Western blottings

Western blotting was done as reported previously.[24] Thirty micrograms of total cell lysate was separated using NuPAGE 4–12% Bis-Tris gels (Invitrogen, CA, USA) and blotted onto an Immobilon polyvinylidene difluoride membrane (Roche). The membrane was incubated with the primary antibodies followed by a peroxidase-labeled anti IgG antibody, and visualized by chemiluminescence reaction (BM Chemiluminescence Blotting Substrate; Roche). The antibodies used were anti-NS5A (BioDesign, ME, USA), anti-core (provided by Dr. Wakita), and anti-beta-actin antibodies (Sigma).

## MTS assays

To evaluate cell viability, MTS (dimethylthiazol carboxymethoxyphenyl sulfophenyl tetrazolium) assays were performed using a Cell Titer 96 Aqueous One Solution Cell Proliferation Assay (Promega) according to manufacturer's directions.

## HCV-JFH1 virus cell culture

An *in vitro* transcribed HCV-JFH1 RNA[25] was transfected into Huh7.5.1 cells.[26] Naïve Huh7.5.1 cells were subsequently infected by culture supernatant of the JFH1-RNA transfected Huh-7.5.1 cells, and subjected to culture in the presence of drugs. Culture medium was collected serially and HCV core antigen was measured using a chemiluminescence enzyme immunoassay (CLEIA) according to the manufacturer's protocol (Lumipulse Ortho HCV Antigen; Ortho-Clinical Diagnostics, Tokyo, Japan). Cellular virus expression was measured by the Western blotting using anti-core antibodies.[27]

## Statistical analyses

Statistical analyses were performed using Student's *t*-test. *P*-values of less than 0.05 were considered statistically significant.